

CRYSTALLIZATION KINETICS OF POLYPROPYLENE-POLYETHYLENE-BASED COPOLYMERS

*J. J. Suñol, J. Saurina, R. Berlanga, D. Herreros, P. Pagès¹ and
F. Carrasco²*

Department of Industrial Engineering, Universitat de Girona, Av. Ll. Santaló s/n, 17071 Girona

¹Department of Materials Science, Universitat Politècnica de Catalunya

²Department of Chemical Engineering, Universitat de Girona, Spain

(Received January 13, 1998)

Abstract

A crystallization kinetics analysis of several polypropylene-polyethylene (PP-PE), PP-rich copolymers was made by means of differential scanning calorimetry. The crystallization was studied via calorimetric measurements at different cooling rates. Several additives were added to the base material. Some test samples were subjected to artificial ageing processes. A modified isoconversional method was used to describe the crystallization process under non-isothermal conditions. The value of the Avrami parameter was determined for primary and secondary crystallization.

Keywords: artificial ageing, DSC, dynamic crystallization, isoconversional method

Introduction

Copolymer materials are widely used in industry because they are economically viable and versatile tools for modification of the properties of polymeric base structures. Nevertheless, due to their sensitivity to degradation and to ageing processes [1-3], pieces need to be replaced recurrently. The processing of thermoplastics always implies cooling within the crystallization temperature interval.

This paper reports a study of the crystallization process from the molten material. To simulate real processes, crystallization was performed in a dynamic regime and cooling was controlled during the experiments.

The use of additives could possibly accelerate the crystallization process. The effects of several additives on the melting and crystallization temperature of polypropylene [4] and on the non-isothermal crystallization of polymers have been studied by means of calorimetric measurements [5-9]. Avrami's equation was used to investigate kinetics under isothermal conditions [10-12] because it

describes the relationship between the crystallized fraction α and time t . Avrami's equation actually describes the kinetics of the set of possible phase transformations, including nucleation and crystalline growth in the isothermal regime:

$$\alpha = 1 - \exp[-k(t)^n] \quad (1)$$

where k is the rate constant of crystallization and n is the Avrami parameter. The value of n indicates the qualitative mechanism governing nucleation and crystalline growth. A variation in parameter n is linked to a change in the mechanism governing the process. In a non-isothermal regime, it is customary to use the following equation:

$$\ln(-\ln(1 - \alpha)) = -\left(\frac{A'}{\beta}\right) \int_{T_0}^T \exp\left(-\frac{E}{RT}\right) dT' \quad (2)$$

where E is the activation energy. To obtain this equation, it is necessary to assume that the crystallization rate constant follows the Arrhenius equation. In our case, we consider another approach to study the problem. The theoretical justification is given in the Results and discussion section.

Experimental

We analysed a polypropylene–polyethylene (PP–PE), PP-rich (~95% in weight) copolymer manufactured by Repsol and marketed as PPR 1042 (melt flow index $MFI=6.5$, fusion temperature 435 K and density 903 kg m^{-3}). Several different commercial additives were added to the base material, namely antioxidants (Tinuvin 327, Tinuvin 770, Tinuvin 770-DF, Bioxid Kronos CL 2220 and Irganox BZ15), anti-UV agents (Quimisorb 144 and Chimisorb 944) and coloring materials (Iagacolor 10401, Elf Tex 415, Cromofstal A3R, Cromofstal DPP-BO and Cinquasia R RT 891D). Two samples A and B were prepared with different combinations of coloring additives, as in usual in industrial processes.

Samples artificially aged or not were analysed. The artificial ageing of some samples was performed in a Xenon test 450 chamber, using a xenon-arc lamp as a light radiation source to simulate natural ageing. Since the time in the chamber was 5000 h, aged samples were denoted A-5000 h and B-5000 h, respectively. Artificial ageing differs from natural ageing; the artificial process was performed under homogeneous conditions, and subsequently thermal stress was not produced. The ageing time simulated was 3 years.

The calorimetric experiments were carried out in a Mettler DSC30 apparatus calibrated by use of the multiple indium, lead and zinc standard. Three types of experiments were carried: heating at a constant rate, an isothermal regime and cooling at a constant rate. First, solid-state material was heated at a constant rate

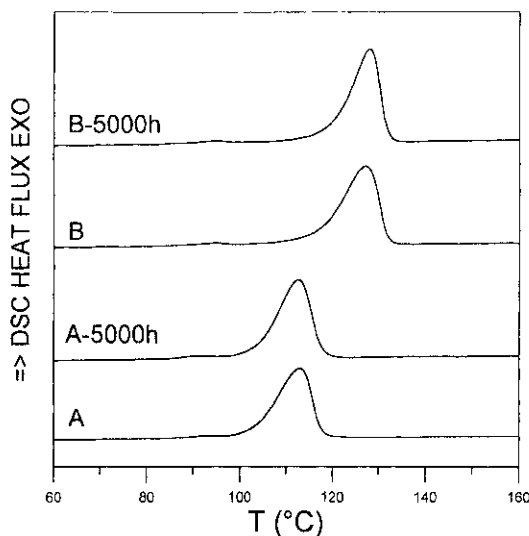


Fig. 1 DSC curves corresponding to samples cooled at 20 K min^{-1} after fusion

of 10 K min^{-1} until it was completely molten. The material was kept liquid under isothermal conditions for 3 min. Next, the experiments were performed at a constant cooling rate of 2.5, 5, 10, 20 or 40 K min^{-1} . Figure 1 shows the DSC curves corresponding to the different samples cooled at 20 K min^{-1} . It can be stated that the artificial ageing produced hardly any relevant changes in the samples. Changes in characteristic temperatures are very sensitive to the use of different coloring additives. Finally, the samples were heated again, but this time at 10 K min^{-1} , to observe the presence and features of the endothermic peak corresponding to melting. Figures 2 and 3 show DSC curves obtained from the treatment of samples A and B. Experiments were repeated at least three times.

Results and discussion

In all cases when the temperature exceeded 200°C , the calorimetric study of the samples verified that different chemical decomposition and oxidation processes occur [8]. The samples were thermally studied by heating them up to a given temperature, and cooling them after an isothermal period. When samples were heated up to 300°C and cooled, no transition was detected. However, when they heated to temperatures between 200 and 300°C , an exothermal process associated with crystallization of the sample was detected, regardless of the cooling rate applied. Nonetheless, the transformation enthalpy decreased with respect to the melting enthalpy. When the samples were heated for the second time, the melting displayed a decrease in enthalpy with respect to the previous exothermal process.

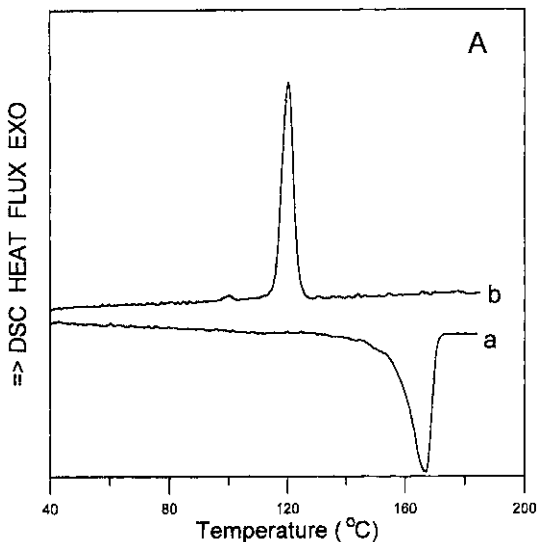


Fig. 2 Sample A. DSC curves obtained: (a) on heating at 10 K min⁻¹, (b) on cooling at 5 K min⁻¹

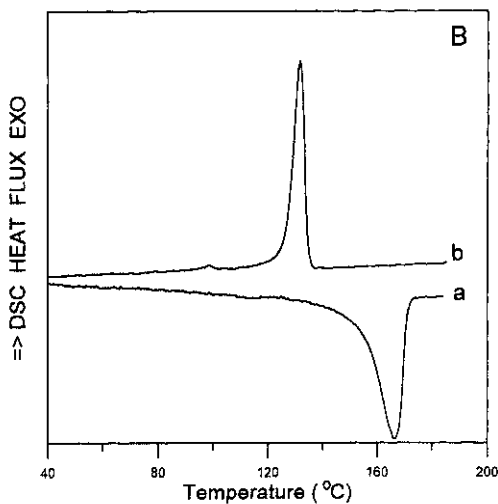


Fig. 3 Sample B. DSC curves obtained: (a) on heating at 10 K min⁻¹, (b) on cooling at 5 K min⁻¹

In contrast, when a sample was heated up to 190°C, in the subsequent cooling the transformation enthalpy showed a slight increase. Moreover, in the subsequent heating, the enthalpy did not change. Table 1 presents some experimental data corresponding to sample B.

Table 1 Melting enthalpy and characteristic temperatures of transitions of sample B

T interval/ °C	Rate/ K min ⁻¹	T_{onset} / °C	T_{peak} / °C	H / J g ⁻¹
25–300	5	156.4	166.0	67.9
	-10	128.1	129.6	–
	5	–	–	–
25–225	5	154.8	164.8	65.2
	-10	133.6	129.6	52.2
	5	142.4	159.1	15.3
25–190	5	155.2	166.7	74.3
	-10	134.8	131.0	84.5
	5	156.4	166.6	86.5

The enthalpy changes relate to samples with different degrees of amorphousness, as occurs in the case of aged samples. The decrease in melting temperature denotes a lower thermal stability of the material.

Let us suppose that, for a given time, the crystalline fraction is proportional to the ratio of the partial crystallization peak area and the total peak area S . The conversion degree achieved can then be determined for this given time from partial consecutive measurements of the crystallization peak area.

In industrial processes, time is a determining factor as concerns cost-effectiveness. Accordingly, time functions are usually included in both non-isothermal and isothermal analyses, independently of the physical meaning. Figure 4 depicts the crystallized fraction, $\alpha(t)$, as a function of $\log t$ for the different samples. The behavior observed in the DSC curves, corresponding to a given material, is very similar, regardless of degradation. The time necessary for an identical crystalline fraction to crystallize is greater in samples A and A-5000h. This may be related to the peculiarities of the rheological character of the flux. These peculiarities arise during the process leading to the production of material and are caused by the presence of different coloring additives. The results on the aged samples can be attributed to the existence of supplementary CO groups, to greater oxidation and to the amount of impurities, all detected by FTIR [13] measurements. Samples B and B-5000h exhibited similar behavior; the ageing did not produce essential changes in the thermal processes of the base material. In the modelling of the crystallization process, we will distinguish cold crystallization, for which the analysis often involves standard methods relating to activation energy [14, 15], and solidification from the melt. The main difference is that cold crystallization of a polymeric mixture may be promoted by pre-existing nuclei. However, solidification from the isotropic melt is expected to be driven by nucleation. In this case, a certain amount of undercooling $\Delta T = T_f - T$, where T_f

is the melting temperature, is necessary to start solidification [16]. Moreover, one expects a rate constant of the approximate form [17]

$$k(T) = A' \exp \left[-\frac{B'}{T} (\Delta T)^2 \right] \quad (3)$$

where A' is a function of temperature, with a slower variation than the exponential factor in a temperature interval $\Delta T \leq 0.3T_f$, and B' is a constant proportional to $\sigma^3/\Delta S_f^2$, where σ is the interfacial energy between the liquid and the nucleus, and ΔS_f is the melting entropy.

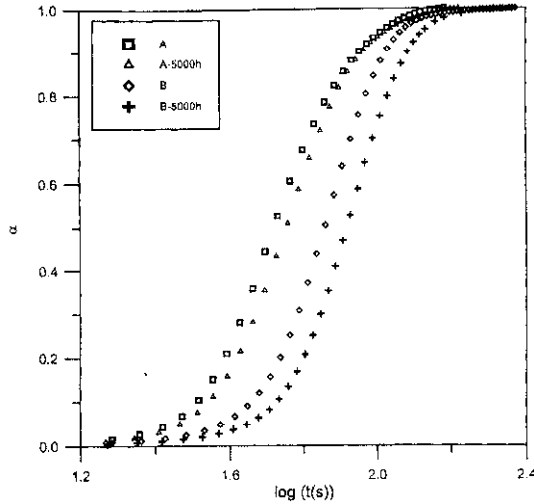


Fig. 4 Crystalline fraction as a function of the logarithm of time for crystallization under non-isothermal conditions

The derivative of Eq. (1) under continuous cooling (or heating) treatment at a constant rate, β , initially introduced by Doyle [18] to derive kinetic data from a thermogravimetric curve, is

$$\frac{d\alpha}{dT} = \frac{kf(\alpha)}{\beta} \quad (4)$$

Under continuous cooling at a constant rate, the integrated form of this equation becomes

$$g(\alpha) = \int_{\alpha_0}^{\alpha} \frac{d\alpha'}{f(\alpha')} = -\frac{A'}{\beta} \int_{T_0}^T \exp \left[-\frac{B'}{T} (\Delta T)^2 \right] dT' \quad (5)$$

where $g(\alpha) = -[\ln(1-\alpha)]^n$. Moreover, we can define $x = B'/T(\Delta T)^2$.

This equation can be rewritten as

$$g(\alpha) = \frac{A' \exp(-x) \int_{T_0}^T \exp(-x) dT'}{\beta x \frac{\exp(-x)}{x}} \tag{6}$$

Moreover, we can define

$$\tau(x) = \frac{x}{\exp(-x)} \int_{T_0}^T \exp(-x) dT' \tag{7}$$

Now, $g(\alpha)$ can be rewritten as

$$g(\alpha) = \frac{-A' \tau(x) \exp(-x)}{\beta x} = \frac{-T(\Delta T)^2 \tau(x) k(T)}{\beta B'} \tag{8}$$

From this equation and $g(\alpha) = -[\ln(1-\alpha)]^n$, the following expression can be deduced:

$$\ln(-\ln(1-\alpha)) = \ln \left[\frac{-T(\Delta T)^2 \tau(x)}{\beta} \right]^n - \frac{nB'}{T} (\Delta T)^2 \tag{9}$$

If it is assumed that $\ln[-T(\Delta T)^2 \tau(x)/\beta]^n \approx \text{constant}$, the slope of $\ln(-\ln(1-\alpha))$ vs. $1/T(\Delta T)^2$ provides nB' for a given α . To find n , it is necessary to know B' .

In other works, the isoconversional method [19, 20] was applied to find the activation energy for a given value of the degree of conversion (α). Here, this method is adapted to evaluate the constant B' in the case of solidification from an isotropic melt [21]. In the knowledge of B' , calculated by a multiple-scan method that requires several measurements at different cooling rates, the slope provides n . As an example, Fig. 5 shows the $\ln(-\ln(1-\alpha))$ dependency of $1/T(\Delta T)^2$ under non-isothermal conditions for sample A. The presence of two zones with clearly different slopes is observed. Table 2 lists the average Avrami parameter n corresponding to the different crystallization stages. The value of the parameter n var-

Table 2 Average Avrami parameter, n , for primary (n_1) and secondary (n_2) crystallization

Sample	n_1	n_2
A	3.9	1.9
A-5000h	4.1	1.7
B	4.0	1.7
B-5000h	4.1	2.0

ies during the crystallization process; such a variation is linked to a change in the mechanism governing the process (assumed in this work to be primary and secondary crystallization).

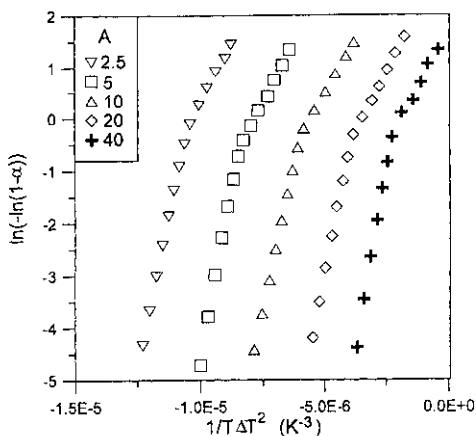


Fig. 5 Dependence of $\ln(-\ln(1-\alpha))$ on $1/T(\Delta T)^2$ at different cooling rates

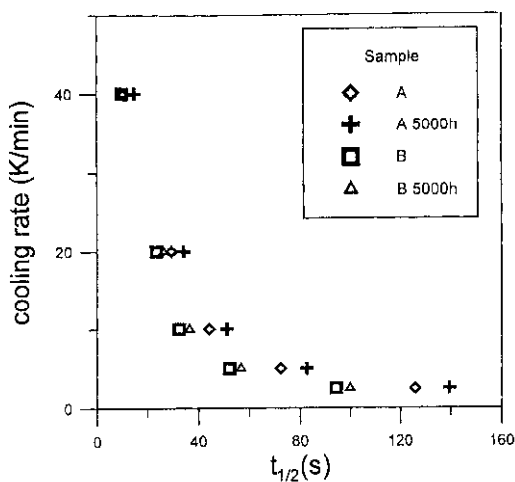


Fig. 6 Average crystallization half-time, $t_{1/2}$, depending on cooling rate

The Avrami parameter obtained by studying the non-isothermal crystallization kinetics during the first stage (primary crystallization) is approximately $n=4$ for all samples at any cooling rate. This value corresponds to three-dimensional nucleation dominated by the interphase [22]. The results obtained at different cooling rates are similar. This fact confirms that the use of different additives and the degree of artificial ageing do not produce significant changes in the

crystallization mechanisms corresponding to the overall crystallization processes. The second stage (secondary crystallization, $n \approx 2$) appears to be more road-like growth with sporadic nucleation than disk-like nucleation.

Figure 6 demonstrates the variation in the crystallization half-time, $t_{1/2}$, with the cooling rate used. As expected, the half-time decreases as the cooling rate does. Sample A is the most sensitive to artificial ageing.

Conclusions

The addition of small amounts of several different additives to polypropylene–polyethylene–based copolymers leads to a decrease in the crystallization rate in the dynamic regime, but no appreciable changes occur in the crystallization mechanisms. The kinetic analysis clearly shows two different regions of crystallization (primary and secondary). The value of the Avrami parameter in zone 1, around 4 for the whole sample, corresponds to three-dimensional nucleation controlled by the interphase. Overall analysis of the results does not reveal a great dependence on the cooling rate. Crystallization half-time measurements indicate that sample A is the most sensitive to artificial ageing.

* * *

This work was partially funded by projects CIRIT GRQ-2048 and UdG N° 9196012.

References

- 1 S. Shivkumar and B. Gallois, *Trans. Am. Foundrymen's Soc.*, 95 (1987) 791.
- 2 M. Rama Rao and T. S. Radhakrishnan, *J. Appl. Polym. Sci.*, 41 (1990) 2251.
- 3 S. Mehta, S. Biederman and S. Shivkumar, *J. Mater. Sci.*, 30 (1995) 2944.
- 4 G. M. Kerch and L. A. Irgen, *Thermochim. Acta*, 93 (1985) 135.
- 5 V. P. Privalko, T. Kawai and Yu. S. Lipatov, *Colloid and Polymer Sci.*, 257 (1979) 1042.
- 6 J. Rychly and I. Janigova, *Thermochim. Acta*, 215 (1993) 211.
- 7 M. Zhang, H. Zeng, Y. He and K. Mai, *Thermochim. Acta*, 257 (1995) 183.
- 8 R. Berlanga, J. Saurina and J. J. Suñol, *Scientia Gerundensis* (1997) accepted.
- 9 R. Berlanga, J. Saurina, M. T. Clavaguera-Mora and N. Clavaguera, II. Jornadas sobre calorimetría y análisis térmico de polímeros. Madrid, 1996.
- 10 M. Avrami, *J. Chem. Phys.*, 7 (1939) 1103.
- 11 A. Sharples, *Introduction to Polymer Crystallization*, Edward Arnold, London, 1966.
- 12 J. J. Suñol, PhD thesis Universitat Autònoma de Barcelona, Barcelona, 1996.
- 13 P. Pagès, F. Carrasco and J. Romeu, *Revista de Plàstics Modernos*, 71 (1996) 475.
- 14 H. E. Kissinger, *Anal. Chem.*, 29 (1957) 1702.
- 15 T. Ozawa, *J. Thermal Anal.*, 2 (1979) 301.
- 16 D. Turnbull, *Contemp. Phys.*, 10 (1969) 473.
- 17 N. Clavaguera, J. Saurina, J. Lheritier, J. Masse, A. Chauvet and M. T. Mora, *Thermochim. Acta*, 290 (1997) 173.
- 18 C. D. Doyle, *J. Appl. Polymer Sci.*, 5 (1961) 285.
- 19 J. Málek, *Thermochim. Acta*, 138 (1989) 337.
- 20 J. M. Criado, J. Málek and A. Ortega, *Thermochim. Acta*, 147 (1989) 377.
- 21 R. Berlanga, J. Farjas, J. Saurina and J. J. Suñol, *Revista de Ciència*, 20 (1997) 7.
- 22 J. W. Christian, in 'Theory of Transformation in Metals and Alloys', Pergamon Press, 1975.